2018

Discrimination of isobaric and isomeric lipids in complex mixtures by combining ultra-high pressure liquid chromatography with collision and ozone-induced dissociation

Amani M. Batarseh
University of Wollongong, amani@uow.edu.au

Sarah K. Abbott
University of Wollongong, sarahmac@uow.edu.au

Eva Duchoslav
SCIEX

Ayedh Alqarni
University of Wollongong, asa043@uowmail.edu.au

Stephen J. Blanksby
Queensland University of Technology, stephen.blanksby@qut.edu.au

See next page for additional authors

Publication Details

Batarseh, A. M., Abbott, S. K., Duchoslav, E., Alqarni, A., Blanksby, S. J. & Mitchell, T. W. (2018). Discrimination of isobaric and isomeric lipids in complex mixtures by combining ultra-high pressure liquid chromatography with collision and ozone-induced dissociation. International Journal of Mass Spectrometry, 431 27-36.

Discrimination of isobaric and isomeric lipids in complex mixtures by combining ultra-high pressure liquid chromatography with collision and ozone-induced dissociation

Abstract

The inability of current mass spectrometry techniques to differentiate phospholipid isomers results in a routine under-estimation of phospholipid molecular diversity in complex biological matrices. Recent technological advances in tandem mass spectrometry and ion activation are helping to overcome these limitations, but all rely on tandem mass spectrometry with unit mass-selection and suffer from co-isolation of isobaric or isomeric species. Accordingly, separation of phospholipid isomers and isobars prior to characterization is required to fully delve into the complexity of the lipidome. Here we present a novel two-stage workflow combining reversed-phase ultra-high performance liquid chromatography with ozone-induced dissociation (OzID) and combined-collision- and ozone-induced-dissociation (COzID) that reduces spectral complexity and enables discrimination of lipid isomers and isobars. Application of this technique to the analysis of human red blood cell lipid extracts allowed the separation, or partial separation, of adduct ion and head group isobars as well as double bond and sn-positional isomers affording near complete structural characterization of low abundance lipids, e.g. PC 18:0/20:3(n-6), PS 18:0/20:4(n-6) and PS 20:4(n-6)/18:0 all observed at m/z 834.7. We also introduce a software plug-in that automatically annotates OzID mass spectra to assign the carbon-carbon double bond positions in lipids. This new workflow allows us to delve deeper into the lipidome and represents another valuable tool for the lipidomics toolbox.

Publication Details

Batarseh, A. M., Abbott, S. K., Duchoslav, E., Alqarni, A., Blanksby, S. J. & Mitchell, T. W. (2018). Discrimination of isobaric and isomeric lipids in complex mixtures by combining ultra-high pressure liquid chromatography with collision and ozone-induced dissociation. International Journal of Mass Spectrometry, 431 27-36.

Authors

Amani M. Batarseh, Sarah K. Abbott, Eva Duchoslav, Ayedh Alqarni, Stephen J. Blanksby, and Todd W. Mitchell

International Journal of Mass Spectrometry 431 (2018) 27–36

Contents lists available at ScienceDirect

International Journal of Mass Spectrometry

journal homepage: www.elsevier.com/locate/ijms

Full Length Article

Discrimination of isobaric and isomeric lipids in complex mixtures by combining ultra-high pressure liquid chromatography with collision and ozone-induced dissociation

Amani M. Batarseh [a,b], Sarah K. Abbott [a,b], Eva Duchoslav [c], Ayedh Alqarni [a,b], Stephen J. Blanksby [d], Todd W. Mitchell [a,b,*]

[a] School of Medicine, Faculty of Science Medicine and Health, University of Wollongong, Wollongong, NSW, Australia
[b] Illawarra Health and Medical Research Institute, Wollongong, NSW, Australia
[c] SCIEX, Concord, ON, Canada
[d] Central Analytical Research Facility, Institute for Future Environments, Queensland University of Technology, Brisbane, QLD, Australia

ARTICLE INFO

Article history:
Received 19 February 2018
Received in revised form 3 May 2018
Accepted 22 May 2018
Available online 26 May 2018

Keywords:
Lipid
Lipidomics
Erythrocytes
Mass spectrometry

ABSTRACT

The inability of current mass spectrometry techniques to differentiate phospholipid isomers results in a routine under-estimation of phospholipid molecular diversity in complex biological matrices. Recent technological advances in tandem mass spectrometry and ion activation are helping to overcome these limitations, but all rely on tandem mass spectrometry with unit mass-selection and suffer from co-isolation of isobaric or isomeric species. Accordingly, separation of phospholipid isomers and isobars prior to characterization is required to fully delve into the complexity of the lipidome. Here we present a novel two-stage workflow combining reversed-phase ultra-high performance liquid chromatography with ozone-induced dissociation (OzID) and combined-collision- and ozone-induced-dissociation (COzID) that reduces spectral complexity and enables discrimination of lipid isomers and isobars. Application of this technique to the analysis of human red blood cell lipid extracts allowed the separation, or partial separation, of adduct ion and head group isobars as well as double bond and *sn*-positional isomers affording near complete structural characterization of low abundance lipids, e.g. PC 18:0/20:3(*n*-6), PS 18:0/20:4(*n*-6) and PS 20:4(*n*-6)/18:0 all observed at *m/z* 834.7. We also introduce a software plug-in that automatically annotates OzID mass spectra to assign the carbon–carbon double bond positions in lipids. This new workflow allows us to delve deeper into the lipidome and represents another valuable tool for the lipidomics toolbox.

1. Introduction

Lipids play important roles in cellular structure and function and understanding these dynamic interactions is a critical focus of the field of lipidomics. Critical to such investigations has been the desire to establish a baseline understanding of what constitutes a lipidome for a particular cell or organism. That is, how many lipids are present and what is their absolute or relative concentration? This seemingly straightforward ambition is challenged by the large differences in concentration of different lipid components and the sheer molecular diversity of lipids; with estimates ranging from several hundred to several hundred thousand individual molecular components [1–3]. Focusing on phospholipids alone, the high potential of isobaric and isomeric overlap between individual lipids is due in part to the numerous combinations of different headgroups and fatty acids that vary in chain length, number and position of double bonds, position of substitution on the glycerol backbone and stereochemistry. These combinations give rise to extensive chemical diversity of biological lipidomes and highlight the challenges in differentiating and uniquely identifying lipids in contemporary workflows [4–9].

Recent advances in mass spectrometry have provided powerful new tools to address the challenges of structural lipidomics [6,10,11]. In particular, enhancements in sensitivity, mass resolving power, speed of analysis, and multi-stage fragmentation have

* Corresponding author at: School of Medicine, Faculty of Science Medicine and Health, University of Wollongong, Wollongong, NSW, Australia.
E-mail addresses: amani@uow.edu.au (A.M. Batarseh), sarahmac@uow.edu.au (S.K. Abbott), eva.duchoslav@sciex.com (E. Duchoslav), asa043@uowmail.edu.au (A. Alqarni), stephen.blanksby@qut.edu.au (S.J. Blanksby), toddm@uow.edu.au (T.W. Mitchell).

https://doi.org/10.1016/j.ijms.2018.05.016
1387-3806/

enabled the development of protocols for identification and quantification of hundreds of lipid species per sample [6,11]. In a recent example, a combination of high resolution mass analysis and collision-induced dissociation (CID) afforded the identification of 300 lipids in one sample [10]. However, even such advanced instrumentation can be limited in resolution of closely spaced isobars and discrimination of lipid isomers [4]. This ultimately limits the molecular description of the lipids and thus the complexity of the lipidome is not fully described. In response, additional mass spectrometric methods aimed at differentiating lipid isomers have evolved; largely targeting double bond positional isomers and *sn*-regioisomers. These include, ozone-induced dissociation (OzID) [8,12,13] alone or coupled with CID [14], electron-induced dissociation (EID) [15], the Patterno-Buchi reaction; [16] and UVPD [17]. The advantages and limitations of these new generation technologies have been recently reviewed [7] but all rely on tandem mass spectrometry with unit mass-selection and can thus suffer from complexity arising from co-isolation of isobaric or isomeric species. Taken together, the aforementioned methods are capable of addressing specific questions in the characterization of lipid structures; however, no one technology in isolation is yet capable of fully unravelling the molecular complexity of the lipidome [7].

Chromatographic or mobility-based separations [18] used in conjunction with new ion activation approaches may offer solutions to the full description of the lipidome. Previously we have demonstrated proof-of-principle protocols combining liquid chromatography (LC) separations with ozone-induced dissociation workflows [19–21]. These approaches were successful in affording partial separation and unique identification of glycerophospholipid isomers in mixtures of synthetic lipids, but were less successful when applied to biological lipid extracts [19,20]. To this point however, complicated lipid mixtures have not been thoroughly examined and the full benefits of chromatographic separations to spectral complexity have not previously been demonstrated. Here, we expand and improve the information that can be gained from LC-OzID workflows and introduce a hybrid protocol we term, combined-collision- and ozone-induced dissociation (COzID), that affords information on both double-bond and *sn*-position in glycerophospholipids. Furthermore, we introduce the application of a novel software plug-in for automating OzID-mass spectral annotations.

The lipidome of human red blood cells (RBC) has previously been discussed as a model system to explore lipid structural diversity [5]. Despite numerous studies however, a full description of even the phosphatidylcholine (PC) class remains elusive [22–25]. Understanding the baseline complexity of human RBC can have wide reaching importance as these cells are widely analyzed as carriers of possible lipid biomarkers in clinical studies [26–28]. While a comprehensive study of the full RBC lipidome is beyond the scope of the present investigation it provides an excellent target for establishing the performance of our protocols for the discrimination and identification of isomeric and isobaric lipids in a cellular lipid extract.

2. Methods

2.1. Materials

All solvents used, including water, were LC–MS grade and purchased from VWR Inc (Tingalpa, QLD, Australia). Butylated hydroxytoluene (BHT) was purchased from Sigma-Aldrich (Castle Hill, NSW, Australia). Ammonium acetate and sodium acetate (analytical grade) were purchased from Ajax Chemicals (Auburn, NSW, Australia). Industrial-grade compressed oxygen with 0.5% nitrogen was obtained from BOC (Cringila, NSW, Australia). Synthetic phospholipids; 1,2-di-(9*Z*-octadecenoyl)-*sn*-glycero-3-phosphocholine (PC 18:1(*n*-9)/18:1(*n*-9)), 1,2-di-(6*Z*-petroselinoyl)-*sn*-glycero-3-phosphocholine (PC 18:1(*n*-12)/18:1(*n*-12)), 1-octadecanoyl-2-(9*Z*,12*Z*-octadecadienoyl)-*sn*-glycerol-3-phosphocholine (PC 18:0/18:2(*n*-6,*n*-9)), 1-(9*Z*-octadecenoyl)-2-octadecanoyl-*sn*-glycero-3-phosphocholine (PC 18:1(*n*-9)/18:0) and 1-octadecanoyl-2-(9*Z*-octadecenoyl)-*sn*-glycero-3-phosphocholine (PC 18:0/18:1(*n*-9)) were acquired from Avanti Polar Lipids (Alabaster, Alabama, USA).

2.2. Lipid extraction

Blood samples were collected from human subjects in accordance with predefined biobanking standards at the University of Wollongong and ethics approval was obtained from the University of Wollongong Human Ethics Research Committee (HE16/016 & HE16/018). Lipid extraction from human red blood cells followed the methyl *tert*-butyl ether (MTBE) protocol of Matyash et al. [29] that was adapted to a liquid handling workstation (Hamilton STAR, Reno, NV, USA) [30]. In brief, 290 μL of aqueous ammonium acetate (150 mM with 2 mM EDTA) was added to the wells of a 2.0 mL, 96-well plate cooled on ice. A 10 μL aliquot of packed red blood cells was added to each well before the plate was vortexed at 800 rpm for 10 mins. Sample plates, solvents and reagents were loaded onto the liquid handling workstation where the following steps were performed. First, 300 μL of methanol was added and the sample mixed prior to standing for 10 mins. Next, 1000 μL of MTBE was added to the samples and mixed for 30 mins before the mixture was allowed to stand for 15 mins to allow phase separation. Following this, 500 μL of the MTBE top phase was removed, placed in glass vials with Teflon caps and stored at −20 °C until mass spectrometric analysis.

2.3. Sample preparation

2.3.1. Direct infusion mass spectrometry

For direct infusion experiments, RBC lipid extracts were diluted 1:50 in methanol containing 1 μM sodium acetate. Mass spectra were acquired using a hybrid triple quadrupole linear ion-trap mass spectrometer (QTRAP5500® system, SCIEX, Concord, ON, Canada) previously modified to incorporate ozone, generated online by an ozone generator (Titan, Absolute Ozone, Alberta, Canada), into the nitrogen collision gas line [12,31]. For direct infusion experiments, diluted lipid extracts were infused at a flow rate of 3 μL min^{-1} through an ESI source in positive mode. Typical source settings were: 5500 V ion spray voltage; source temperature 250 °C; 100 V de-clustering potential; 10 V for the entrance potential; nitrogen serving as the nebulizing gas at 20 psi; curtain gas 10 psi; and auxiliary gas 20 psi. Typical OzID experimental conditions utilized an oxygen flow rate through the generator of 250 mL min^{-1} with the ozone generator power output at 40% to obtain approximately 220 g Nm^{-3} of ozone (*ca.* 15% v/v ozone in oxygen). The gas flow from the generator was split to direct the majority of the flow through an ozone destruct catalyst (IN USA, Norwood, MA, USA). The remainder was passed through a variable leak valve (VSE Vacuum Technology, Lustenau, Austria) for regulating ozone (in oxygen) introduction into the collision cell (q_2) via the nitrogen collision gas line. An external ambient ozone monitor (Mini-HiCon, IN USA, Norwood, MA, USA) was interlocked to the remote shut-off on the generator and set to disable ozone production if the ambient ozone concentration rose above 60 ppb. All experiments were controlled and data acquired using Analyst® software (SCIEX, Concord, ON, Canada). Direct infusion COzID spectra were acquired by mass selecting precursor ions in the first quadrupole (q1) with an isolation width of 1 Th and accelerating them into q_2 with collision energy of 37 eV. Ions were trapped in the presence of ozone in q2

for 4000 ms. Product ions were then transferred with a post collision energy of 8 eV and measured in the linear ion trap (q_3) with a fill time of 500 ms. Direct infusion spectra are reported here as a summation of 200 cycles (~17.9 mins of spectral acquisition as calculated by Analyst software).

2.3.2. Liquid-chromatography mass spectrometry

For liquid chromatography, a pooled sample from at least 5 different individual RBC lipid extracts was prepared. 200 μL aliquots from the pooled extract were dried down and reconstituted in 200 μL methanol prior to analysis Reversed-phase ultra-high performance liquid chromatography (RP-UHPLC) runs were performed using an UHPLC system (ACQUITY UPLC, Waters, Milford, Massachusetts, USA) fitted with a C_{30} column (Acclaim 2.1 × 150 mm, 3 μm particle size, Thermo Fisher Scientific, Scoresby, VIC, Australia) held at 25 °C. Two mobile phases were used; A: 5 mM ammonium acetate in water, and B: 5 mM ammonium acetate in methanol/acetonitrile (60/40 v/v). The gradient used was 12.5% A to 100% B in 25 min, hold from 25 to 30 min at 100% B, return to 12.5% A over 1 min followed by equilibration for an additional 9 min. For LC–MS operation, 5 μL of sample was injected on column with a solvent flow rate of 500 μL min^{-1}. Sodium acetate (0.5 mM) was infused into the flow path prior to the ESI source using a T-junction at a rate of 15 μL min^{-1}. Ion spray voltage was 5500 V, declustering potential 90 V, entrance potential 8 V and source temperature set to 400 °C. Nitrogen was used as the nebulizing gas at 60 psi pressure, curtain gas 10 psi, and auxiliary gas 30 psi. OzID (for determining double bond position) used entrance to q_2 collision energy of 5–10 eV, linear ion trap fill time of 5 ms, exit collision energy of 8 eV and residence time with ozone of 2000 ms. COzID (for determining *sn*-position) used similar MS parameters except for a modified q_2 collision energy (38–40 eV) and a residence time with ozone of 250 ms.

2.3.3. Data analysis

Spectra were analyzed using PeakView® software (SCIEX, Concord, ON, Canada) with an incorporated OzID plug-in, which allowed for automated annotation of OzID double bond ions. The plug-in works by highlighting the precursor ion of interest from which OzID ions were generated, and manual input of the lipid sum composition into the software (*e.g.,* for $[PC\ 36:1+Na]^+$, *m/z* 810 is highlighted in the spectrum and PC 36:1 is entered in the software). The plug-in searches a database of expected OzID neutral losses and annotates the OzID spectra. Settings concerning the threshold and mass tolerance are used to fine-tune the assignments, and to reduce false annotations. The presence of the aldehyde and Criegee ion pair for each double bond was a requirement for accepting a positive identification. Output was manually curated for correct assignments, and incorrect assignments were removed. An amended nomenclature for labeling the double bond ions as used in this manuscript is explained below.

2.3.4. Nomenclature

Lipid structure nomenclature used here is guided by literature recommendations of Fahy et al. and Liebisch et al. [32,33] with modifications for the OzID plug-in assignments. Double bond location in the IUPAC annotation is indicated by a number, counting from the carboxylic acid end, followed with Z/E indicating *cis*/*trans* isomerism. In this work, the site(s) of unsaturation is indicated to be x-positions from the methyl end by the traditional nomenclature "*n*-x", where "*n*" refers to the number of carbon atoms in the chain and subtracting "x" provides the location of the double bond, for example, PC 18 0/18:2 (9Z,12Z) is represented as PC 18:0/18:2(*n*-6, *n*-9). This nomenclature is instructive in OzID analysis as the observed neutral losses are common to all lipids with double bonds in the same position relative to the highest numbered carbon on the alkyl chain [34]. The ozone reaction results in a pair of ions (aldehyde and Criegee) for each double bond [8,13], and using the OzID plug in, this will be indicated in the assignments as "*n*-x, aldehyde or *n*-x, Criegee". For double bonds in polyunsaturated fatty acids (PUFA), there is an additional number added in the assignment for all bonds except the first to indicate their position in the series. For example: an *n*-9 double bond in *n*-3 20:5 PUFA, would be characterized by ions generated from two neutral loss (NL) transitions (–106 Da and −90Da) [8], and the annotation of the double bond would be(*n*-9,3, aldehyde) and (*n*-9,3, Criegee) respectively, where (9) indicates the site of unsaturation, (3) indicates that it is the third double bond in the series from the methyl end after *n*-3 and *n*-6 double bonds. The first double bond in a series has the double bond site of unsaturation and aldehyde/Criegee. For example, an *n*-3 in the *n*-3 20:5 PUFA would have two NL transitions (–26 Da and −10 Da) and is labelled as (*n*-3, aldehyde) and (*n*-3 Criegee). Double bonds in monounsaturated fatty acids (MUFA) are labelled the same as the first double bond in a series. The stereochemical configuration of the carbon–carbon double bonds was not determined and thus is not indicated.

3. Results and discussion

3.1. Examination of targeted lipid ions from direct infusion of a red blood cell extract

To examine the potential lipid complexity of red blood cells (RBC), lipid extracts were spiked with sodium acetate and directly infused into a specialized electrospray ionization triple quadrupole mass spectrometer operated in positive ion mode. As expected, abundant ions were observed in the region *m/z* 650–900 corresponding to ionized phospholipids. Nominal mass of the most abundant ions in this region were consistent with the $[M+Na]^+$ ions of phosphatidylcholines (PC). Previously described modifications [12,13] to the instrument enable the addition of ozone (*ca.* 15% in oxygen) to the collision region and thus the selected ions were subjected to activation by a combination of collision- and ozone-induced dissociation (COzID). The resulting product ions were mass-analyzed by the third quadrupole operating as a linear ion trap generating a composite spectrum with peaks arising from both processes. Spectra obtained from mass selection of the *m/z*808 and *m/z* 810 precursor ions from the red blood cell extract using the COzID approach are shown in Fig. 1(A) and (B), respectively.

Shotgun workflows are powerful approaches to lipid structural assignment. In complex extracts however, they are challenged by the overlap of multiple lipid isomers and isobars at a given *m/z*, confounding the data analysis. The spectrum shown in Fig. 1(A) reveals a rich fragmentation pattern that results from CID, OzID and a combination of these processes that provide critical information as to the structures of different lipid isobars and isomers. Examining the low mass end of the spectrum, product ions are observed at *m/z* 147 (loss of $C_2H_5O_4NaP$) [35,36] and *m/z* 184 (phosphocholine moiety) [37], corresponding to known CID product ions for PC lipids when ionized in the $[M+Na]^+$ and $[M+H]^+$ forms, respectively. These data indicate the presence of $[PC\ 36:2+Na]^+$, and $[PC\ 38:5+H]^+$. Exact masses of these ions are 808.5827 and 808.5851 such that resolving power of >300,000 would be required to discriminate between them and co-isolation for tandem mass spectral analysis is inevitable. Similar CID ions are found in Fig. 1(B) for *m/z* 810, indicating the presence of ions originating from both $[PC\ 36:1+Na]^+$ and $[PC\ 38:4+H]^+$.

3.1.1. Lipid class isobars

Lipids from different classes can also be present at both *m/z* 808 and 810, which are isobaric on a unit resolution instrument and cannot be separated due to the small differences in mass. For example,

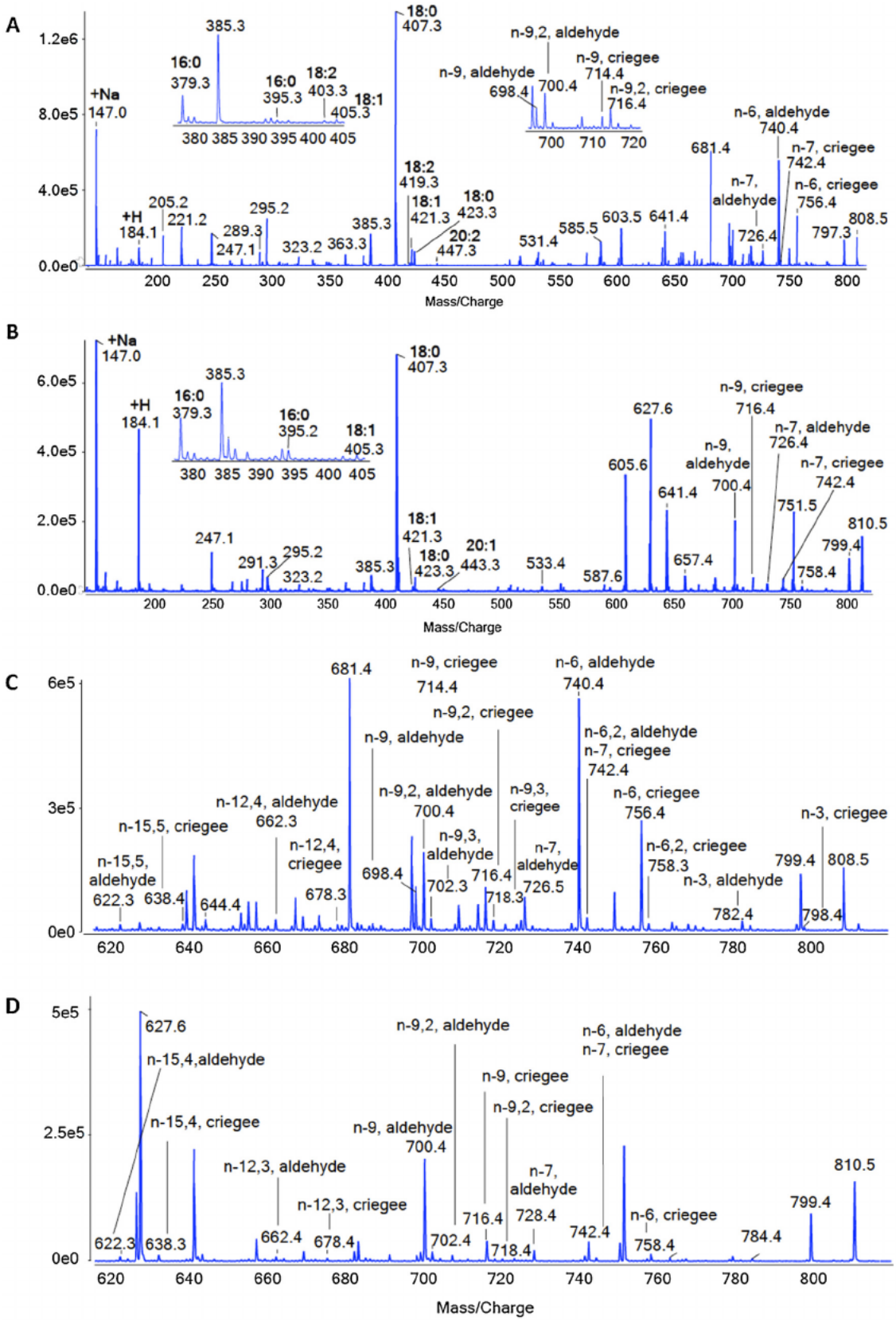

Fig. 1. Direct infusion COzID spectra of RBC lipid extracts. Spectra of (A) *m/z* 808 dominated by $[PC\ 36:2+Na]^+$ ions and (B) *m/z* 810 dominated by $[PC\ 36:1+Na]^+$ ions. Product ions facilitating the assignment of a fatty acyl chain to an *sn*-position in the sodium adduct are shown in bold letters. Product ions arising from the oxidative cleavage of carbon–carbon double bonds are annotated by a software plug-in with respect to (A) $[PC\ 36:2+Na]^+$ and (B) $[PC\ 36:1\ +Na]^+$. Magnification of these spectra across *m/z* 620–820 are shown in panels (C) and (D). OzID product ions are annotated with respect to the precursor ions (C) $[PC\ 38:5+H]^+$ at *m/z* 808 and (D) $[PC\ 38:4+H]^+$ at *m/z* 810.

$[PS\ 36:2+Na]^+$ (m/z 810.5256) overlaps with $[PC\ 36:1+Na]^+$ (m/z 810.5983). Previous data indicates PS 36:2 is present in human RBCs [25] and this is supported by the presence of an ion at m/z 625 (Fig. 1(B and D)) that may have arisen from the loss of the phosphoserine head group (185 Da). Nevertheless, there are no other unique ions present in this spectrum to permit the unequivocal identification of PS36:2 in this RBC lipid extract. If not addressed, this leads to underestimation of the diversity of the RBC phospholipidome.

3.1.2. sn-*Positional isomers*

Another challenge faced in direct infusion protocols is the inability to separate and unambiguously resolve lipid *sn*-positional isomerism, *i.e.*, glycerolipid isomers arising from different sites of substitution of the glycerol backbone. CID of $[PC\ 36:2+Na]^+$ (m/z 808.5827) produced the $[PC\ 36:2+Na\text{-}183]^+$ ion, at m/z 625.5, which, when allowed to react with ozone for 4000 ms, produced ions at m/z 407 and 423 (Fig. 1A). These ions can be used to assign 18:0 at *sn*-1, thus identifying the presence of PC 18:0/18:2 in the extract [20,21]. The presence of low-abundance ions at m/z 403 and 419 ions, indicate that PC 18:2/18:0 is also present in the RBC lipid extract. Ions at m/z 379, 405 and 447 are a result of predicted neutral losses and enable the assignment of acyl chains 16:0, 18:1 and 20:2 at the *sn*-1 position, respectively, in agreement with previous findings (supplementary information, Table S3 and S4) [14,20,21] Taken together, these data indicate the presence of three additional isomers for PC 36:2, *i.e.*, PC 16:0/20:2, PC 20:2/16:0 and PC 18:1/18:1, bringing the total to a minimum of 5 fatty acyl chain- and *sn*-isomers of PC 36:2 in the RBC lipid extract. The same principles can be applied to interrogating the shotgun spectrum for the monounsaturated $[PC\ 36:1+Na]^+$ shown in Fig. 1(B). Similar lipid isomer and isobars are observed, where $[PC\ 36:1+Na]^+$ overlaps with $[PC\ 38:4+H]^+$ as shown by the diagnostic product ions m/z 147 and 184, respectively (Fig. 1(B)). Product ions at m/z 379, 405 407 and 443 indicate the presence of PC 36:1 isomers with 16:0, 18:1, 18:0 and 20:1 fatty acyl chains at the *sn*-1 position thus indicating that this lipid population is comprised of a minimum of four isomers comprised of different acyl chains and *sn*-positions, *i.e.*, PC 16:0/20:1, PC 20:1/16:0, PC 18:0/18:1 and PC 18:1/18:0. Double bond positional isomers are also evident as discussed below.

3.1.3. *Double bond isomers*

OzID ions indicative of double bond position were annotated using the software plug-in developed for our workflow as demonstrated in Fig. 1. The software plug-in is able to assign the double bond positions for both the sodiated and protonated OzID product ions. The spectra were analyzed twice, once for sodiated PC 36:2 or PC 36:1, shown in Fig. 1(A) and (B) respectively, and a second time for protonated PC 38:5 or PC 38:4, shown in Fig. 1(C) and (D) respectively. Numerous double bond isomers of $[PC\ 36:2+Na]^+$ (m/z 808) were detected as shown in Fig. 1(A). The ion pair m/z 740 (–68 Da) and 756 (–52 Da) indicate an *n*-6 double bond, and an additional pair of ions at m/z 700 (–108 Da) and 716 (–92 Da) are indicative of an *n*-9,2 double bond (refer to Table S2 in Supplementary Information). These ions can be assigned to the fatty acyl chains 18:2(*n*-6, *n*-9) or 20:2(*n*-6, *n*-9) for $[PC\ 36:2+Na]^+$, as previously reported [19,21]. Furthermore, double bond isomers from monounsaturated fatty acids (MUFA) are identified by OzID product ions observed at m/z 698 (–110 Da) and 714 (–94 Da) characteristic of an *n*-9 MUFA and m/z 726 (–82 Da) and 742 (–66 Da) ion pair characteristic of an *n*-7 MUFA (Table S1 in Supporting Information) [8,38]. These ions indicate the possibility of at least two, and possibly three double bond isomers namely, PC 18:1(*n*-9)/18:1(*n*-9), PC 18:1(*n*-7)/18:1(*n*-7) and PC 18:1(*n*-7)_18:1(*n*-9).

Fig. 1(C) shows a magnified view of the m/z 610–820 region of the same spectrum displayed in Fig. 1(A). In this instance however, it has been reanalyzed with protonated PC 38:5 as the input precursor ion for the OzID plug-in. Notably, a series of aldehyde and Criegee OzID ion pairs originating from m/z 808, *i.e.*, m/z 782 and 798, m/z 742 and 758, m/z 702 and 718, m/z 662 and 678 and m/z622 and 638 are present. These ions cannot be attributed to any fatty acyl chains in PC 36:2, but can be attributed to a 20:5(*n*-3) polyunsaturated fatty acyl chain of protonated PC 18:0/20:5 (OzID neutral loss transitions are provided in Table S2 in Supporting Information) [8,19]. It is worth mentioning that the aldehyde ion for the *n*-6,2 double bond of an *n*-3 PUFA would overlap with the *n*-7 Criegee ion of a MUFA for that same precursor mass in direct infusion protocols, which would complicate the assignment. Evidence for an *n*-9 double bond in a MUFA is found in Fig. 1(C) and can originate from a monounsaturated fatty acyl chain in PC 38:5 or PC 36:2. The presence of a PC 18:0/20:5 was verified by COzID of the sodiated adduct in positive mode and CID of the $[PC+OAc]^-$ adduct in negative mode (data not shown).

3.2. *Optimization of LC-OzID/COzID workflow*

Fig. 1 demonstrates some of the challenges in obtaining unambiguous structural information on lipids derived from complex biological extracts using a direct infusion COzID approach. To maximise the lipid structural information that can be derived, we investigated the advantages of incorporating LC separation to reduce the complexity. To best match the instrument duty cycle for the LC workflow, we developed two sets of instrument conditions to enhance the abundance of structural diagnostic ion populations for double bond position (OzID) and for *sn*-position (COzID). Optimization of ozone reaction times to generate diagnostic ions on a chromatographic time scale and acquiring sufficient data points across the chromatographic peak was required. The result was to undertake two sample injections in series using the same RP-UHPLC method but operating the MS with optimized protocols for OzID and COzID, respectively. The experiments were first optimized on commercially available synthetic lipids with representative data shown in Figs. 2 and 3. Fig. 2(A) shows an LC chromatogram obtained from injecting an equimolar solution of the three synthetic phosphatidylcholine isomers, PC 18:1(*n*-9)/18:1(*n*-9), PC 18:1(*n*-12)/18:1(*n*-12) and PC 18:0/18:2(*n*-6, *n*-9), onto a reversed-phase C_{30}-column with the addition of sodium acetate post-column. OzID spectra for the selected precursor ions at m/z 808 were obtained with a ~2000 ms residence time in the collision cell. The total ion chromatogram (TIC) constructed from the abundance of all ions detected in OzID scans is shown in Fig. 2(A) revealing two baseline resolved chromatographic features with peak maxima at 23.3 and 25.0 mins.

The extracted-ion chromatograms (XICs) shown in Fig. 2(B) were obtained using product ions diagnostic for different double bond positions namely, m/z 698 (–110 Da, *n*-9) labelled peak 1, and m/z 656 (–152 Da, *n*-12) and m/z 740 (–68 Da, *n*-6) both labelled as peak 2 since they are not fully resolved. In agreement with previous findings, PC 18:1(*n*-9)/18:1(*n*-9) eluted before PC 18:1(*n*-12)/18:1(*n*-12) [19,21]. Although the second feature contains two co-eluting isomers that are not chromatographically resolved, the unique OzID product ions for (*n*-12) and (*n*-6) double bonds, allowed generation of distinct XICs that clearly identified the presence of the two isomers. OzID spectra obtained from integration across chromatographic peaks 1 and 2 (Fig. 2B) are shown in Fig. 2(C) and (D), respectively. Product ions at m/z 698 and 714 dominate the spectrum obtained from the ions eluting at peak 1 (Fig. 2C). These ions are diagnostic for an *n*-9 double bond and confirm PC 18:1(*n*-9)/18:1(*n*-9) as the lipid eluting at 23.3 min. The integrated spectrum obtained from the second peak (Fig. 2D) contains three pairs of product ions, m/z 740 and 756 and m/z 700 and 716 that can be assigned to PC 18:0/18:2(*n*-6, *n*-9) as well as an ion

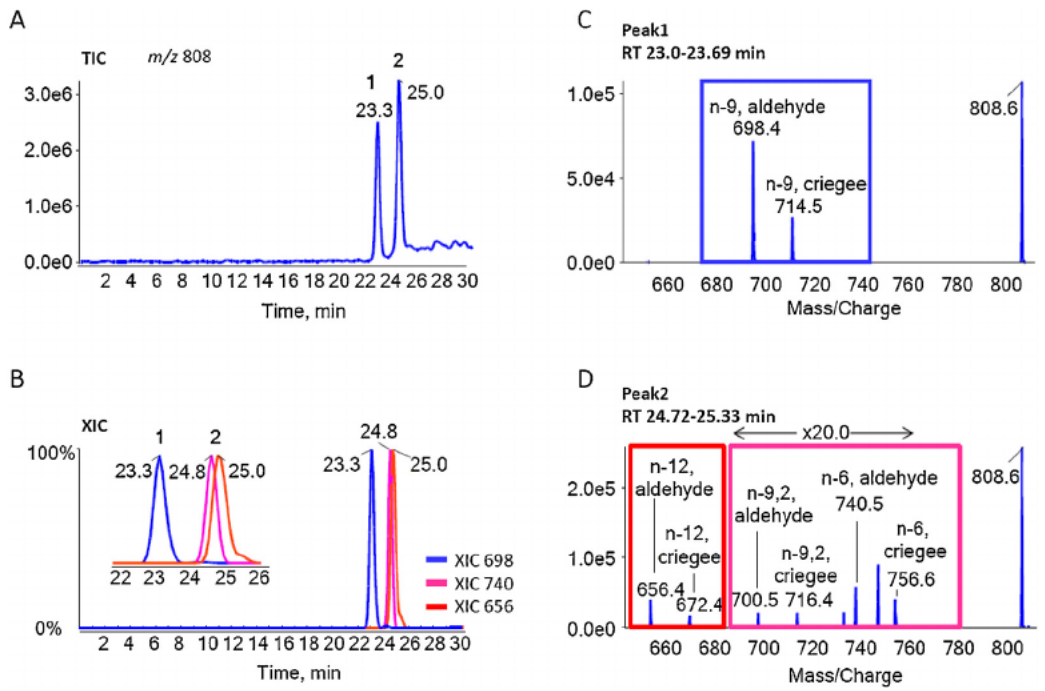

Fig. 2. (A) UHPLC-OzID chromatogram of a 5 μL injection of a mixture of synthetic phosphatidylcholine isomers PC 18:1(*n*-9)/18:1(*n*-9), PC 18:1(*n*-12)/18:1(*n*-12) and PC 18:0/18:2(*n*-6,9). Total ion current for *m*/*z* 808 $[PC\ 36:2+Na]^+$ precursor ions shows two chromatographic features. (B) XICs are shown for OzID product ions from oxidative cleavage of *n*-9 double bond (blue trace) peak #1, two overlapping peaks *n*-6 (pink trace) and *n*-12 (red trace) double bonds, both in peak 2, (expanded in inset). Average OzID mass spectra of the chromatographic features between (C) 23.00-23.69 mins (peak 1) and (D) 24.72-25.33 mins (Peak 2) are shown, and OzID ions for double bonds are annotated using the softwareplug in. (For interpretation of the references to colour in this figure legend, the reader is referred to the web version of this article.)

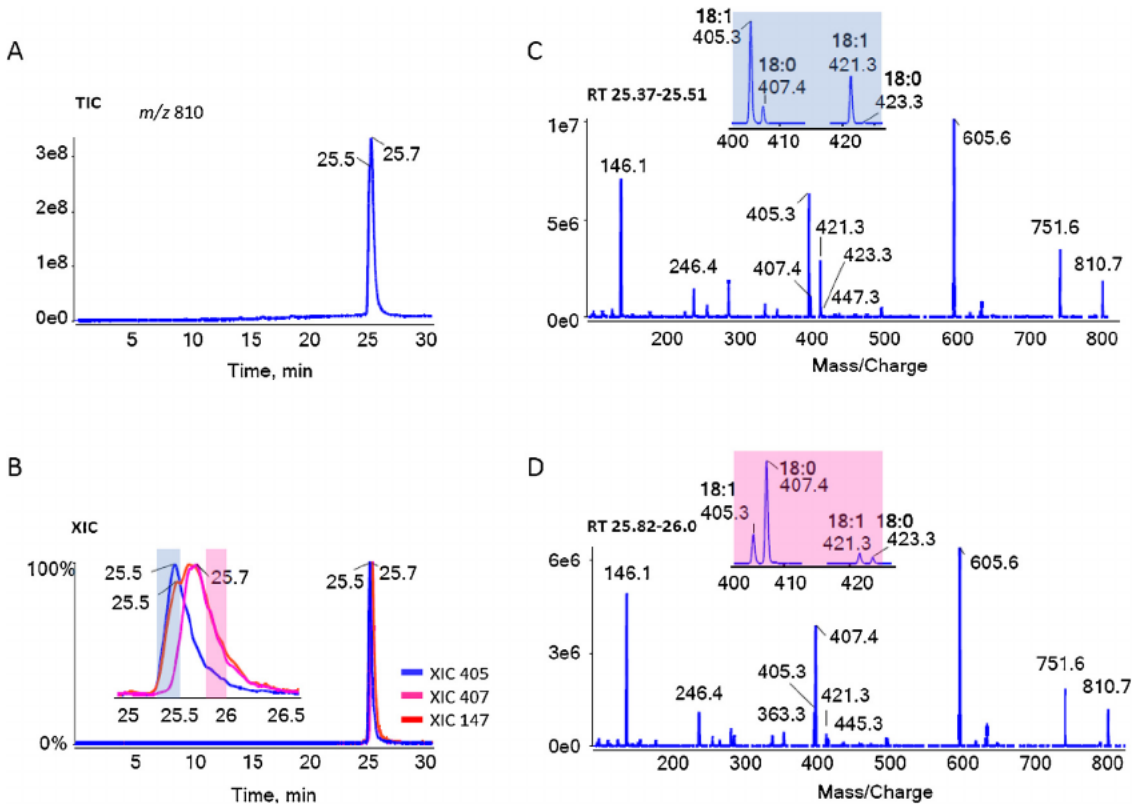

Fig. 3. (A) UHPLC-COzID chromatogram of a 5 μL injection of a mixture of synthetic PC 18:1(*n*-9)/18:0 and PC 18:0/18:1(*n*-9) isomers. Total ion current for *m*/*z* 810 $[PC\ 36:1+Na]^+$ precursor ions shows one chromatographic feature. (B) XICs for CID ion at *m*/*z* 147 (red trace) and COzID diagnostic product ions corresponding to 18:1at *sn*–1 *m*/*z* 405 ion (blue trace), and 18:0 at *sn*–1 *m*/*z* 407 ion (pink trace), expanded in inset. COzID mass spectra obtained by averaging between (C) 25.37-25.51 mins and (D) 25.82-26.00 mins are shown. Annotations of *sn*-positions are shown in bold letters. Insets in (C) and (D) highlight the different ratios in abundance of *m*/*z* 405 and 407 ions at the beginning of the chromatographic peak versus the end. (For interpretation of the references to colour in this figure legend, the reader is referred to the web version of this article.)

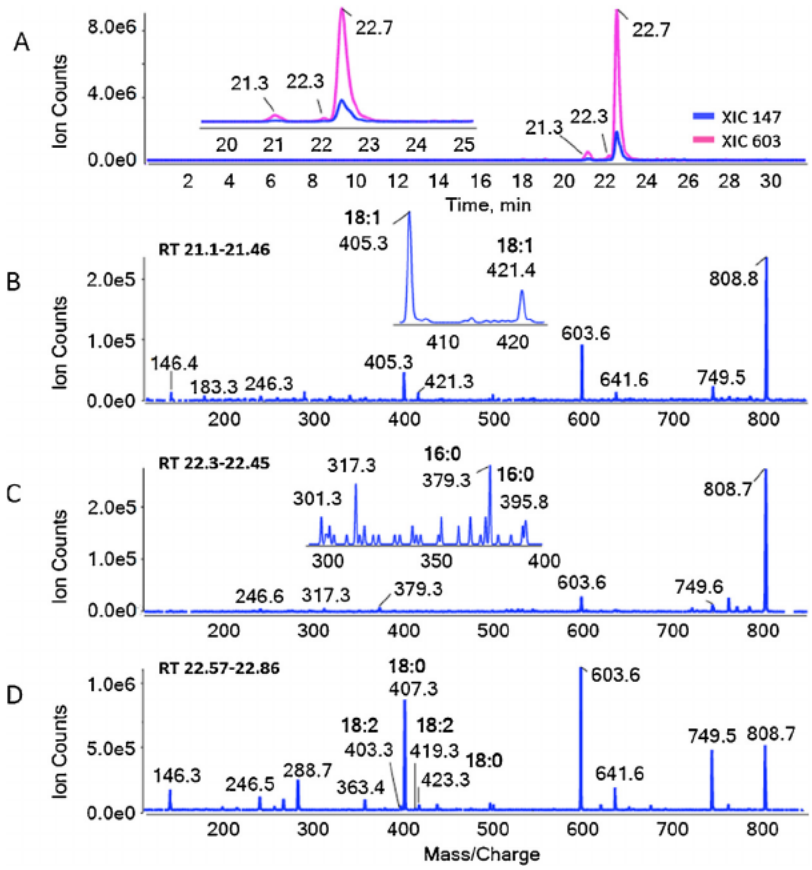

Fig. 4. (A) UHPLC-COzID analysis targeting ions at *m/z* 808 from generated from a 5 μL injection of red blood cell lipid extract. XICs for CID ions *m/z* 147 (blue trace) and 603 $[PC\ 36:2\text{-}Na\text{-}183]^+$ (pink trace) show three chromatographic features (see magnification inset). COzID mass spectra were obtained by integrating between (B) 21.10-21.46 mins, (C) 22.30-22.45 mins and (D) 22.57-22.86 mins. Bold labels show *sn*-1 assignments. (For interpretation of the references to colour in this figure legend, the reader is referred to the web version of this article.)

pair at *m/z* 656 and 672 that correspond to an *n*-12 double bond that can be assigned to PC 18:1(*n*-12)/18:1(*n*-12).

Fig. 3 shows the data obtained from an equimolar mixture of synthetic PC 18:0/18:1(*n*-9) and PC 18:1(*n*-9)/18:0. In these experiments the first quadrupole of the MS was set to transmit ions at *m/z* 810 that were then subjected to conditions optimized for COzID. The TIC of the precursor ion signal at *m/z* 810 is shown in Fig. 3(A), and reveals a single feature with a maximum at 25.7 mins but with a subtle peak shoulder at *ca.* 25.5 mins. The chromatogram in Fig. 3(B) plots the XICs obtained from the COzID product ions *m/z* 405 (assigning 18:1 to the *sn*-1 position) and *m/z* 407 (assigning 18:0 to the *sn*-1 position). Close inspection of these XICs reveals two partially separated peaks with PC 18:1/18:0 eluting slightly earlier than PC 18:0/18:1 (see Fig. 3B, inset). Integrating the spectra obtained at the beginning of the peak (blue box; RT 25.37-25.51 mins) and towards the end of the peak (pink box; RT 25.82-26.00 mins) produces the spectra shown in Fig. 3C and D, respectively. Two COzID product ion pairs at *m/z* 405 and 421 and *m/z* 407 and 423 are present in both spectra and indicate both 18:1 and 18:0 at the *sn*-1 position, respectively. Product ions indicative of an 18:1 at *sn*-1 are higher in abundance in Fig. 3(C), while product ions indicative of an 18:0 at *sn*-1 are higher in Fig. 3(D) (see insets). Therefore, COzID ion ratios confirm that PC 18:0/18:1 elutes just prior to PC 18:1/18:0 indicative of partial separation of these *sn*-positional isomers on the C_{30}-reversed phase column.

3.3. LC-COzID and LC-OzID of RBC lipid extracts

3.3.1. Resolving sn-positional isomers

Data presented in Fig. 4 were acquired by loading 5 μL of RBC lipid extract onto a C_{30}-column and introducing the eluent into the MS through an ESI source operated in positive mode. Data were acquired by mass-selecting ions of *m/z* 808, activating them with a collision energy of 38–40 eV, and trapping both precursor ions and CID products in the presence of ozone for 250 ms yielding COzID mass spectra. The XIC of the *m/z* 147 and 603 product ions, that are characteristic of sodiated PC, are shown in Fig. 4(A) and reveal three peaks with maxima at 21.3, 22.3 and 22.7 mins (see inset). Mass spectra obtained by integrating across each of these three peaks are presented in Fig. 4(B)–(D) and show the expected CID product ions at *m/z* 749 (loss of trimethylamine) and 603 (loss of a sodiated PC headgroup) confirming the identity of each as a phosphatidylcholine. The spectrum obtained from the peak at 21.3 mins (Fig. 4B) shows a single COzID ion pair *m/z* 405 and 421 characteristic of 18:1 at *sn*-1, and can thus be attributed to PC 18:1/18:1. The second chromatographic feature at 22.3 mins (Fig. 4C) contains COzID ions at *m/z* 379 and 395 indicative of 16:0 at *sn*-1 and *m/z* 301 and 317 revealing the presence of 20:2 at *sn*-2 and thus identifies PC 16:0/20:2 (see Tables S3 and S4 in Supporting Information). The COzID spectrum obtained from the third chromatographic feature at 22.7 mins contains ions at *m/z* 407 and 423 identifying 18:0 at *sn*-1 as well as lower abundance *m/z* 403 and 419 ions characteristic of 18:2 at *sn*-1. Taken together, these ions indicate the presence of at least four isomers for PC 36:2; PC 18:1/18:1, PC 16:0/20:2,

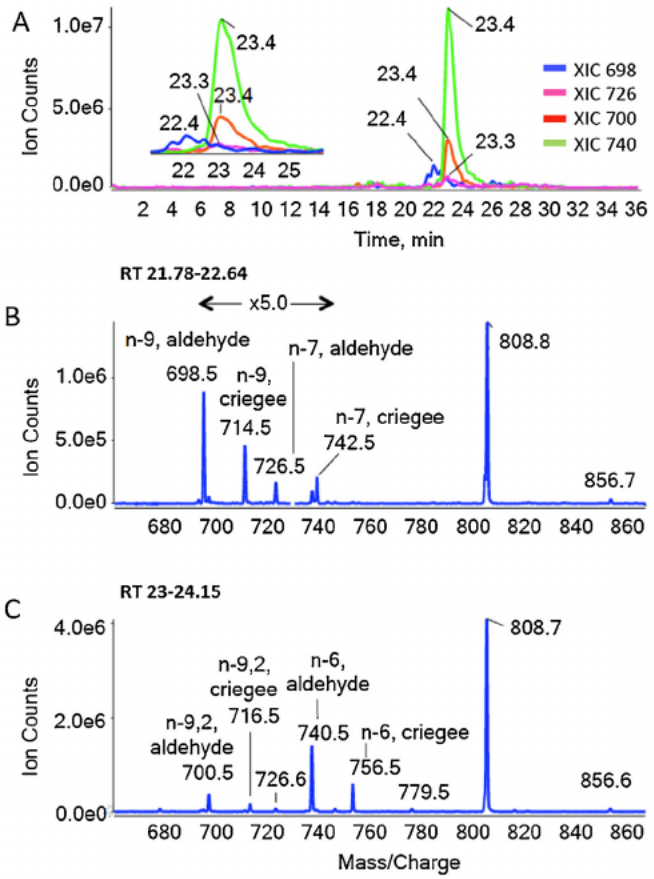

Fig. 5. (A) UHPLC-OzID chromatogram targeting ions at *m/z* 808 from generated from a 5 μL injection of red blood cell extract. [PC 36:2 +Na]$^+$ chromatogram is visualized using XIC for OzID product ions from oxidative cleavage of *n*-9 (blue trace), *n*-7 (pink trace), *n*-9,2 (red trace) and *n*-6 (green trace) double bonds, showing multiple features. OzID mass spectra corresponding to chromatographic features between (B) 21.78-22.64 mins and (C) 23.00–24.15 mins are shown. OzID-ion pairs for double bonds are annotated using the custom PeakView software plug in. (For interpretation of the references to colour in this figure legend, the reader is referred to the web version of this article.)

PC 18:0/18:2 and PC 18:2/18:0. Similar to the PC 36:2 standards, PC 18:1/18:1 is chromatographically resolved from PC 18:0/18:2 in RBC lipid extracts, which simplifies the structural analysis by interrogating each chromatographic peak independently.

3.3.2. Resolving double bond positional isomers

Further analysis of the same population of phosphatidylcholine isomers was undertaken using identical chromatographic conditions but modifying the mass spectrometric conditions for amplification of signals related to carbon–carbon double bond location. In these experiments the *m/z* 808 ions from RBC lipid extracts were mass-selected and delivered to the second quadrupole with lower collision energy (5–10 eV) with subsequent trapping of the ions with ozone for 2000 ms yielding mass spectra with a greater proportion of OzID product ions. Fig. 5 shows representative data acquired under these LC-OzID conditions. XICs of ions diagnostic of PC 36:2 double bond positions are shown in Fig. 5(A) and reveal two main features with maxima at *ca.* 22.4 and 23.4 mins. OzID product ions obtained from the ions eluting at 22.4 mins are observed at *m/z* 698 and 714 in Fig. 5B and correspond to neutral losses of 110 and 94 expected for an *n*-9 double bond. An additional ion pair at *m/z* 726 and 742 corresponding to neutral losses of 82 Da and 66 Da, respectively identify the presence of an *n*-7 double bond. When these data are taken together with the LC-COzID results (see above) they suggest at least two, but up to four possible PC 18:1_18:1 isomers are present in the RBC extract, namely, PC 18:1(*n*-9)/18:1(*n*-9), PC 18:1(*n*-7)/18:1(*n*-7), PC 18:1(*n*-9)/18:1(*n*-7) and PC 18:1(*n*-7)/18:1(*n*-9). Recent work from our group reported the existence of these same four isomers in egg yolk extract, where despite not being separated chromatographically, they were identified using OzID ions [21]. It should be noted that elution of these PC 36:2 species is centered at 22.4 mins in the LC-OzID analysis (Fig. 5A) but the corresponding feature has a maxima at 21.3 min in the LC-COzID analysis (Fig. 4A). This shift in retention time is a consequence of experiments being conducted on different days as there is no shift in retention time when LC-COzID and LC-OzID experiments run on the same day (*cf.* Fig. 4A and Fig. S1A). Regardless, the fidelity of retention time is maintained and therefore such shifts do not limit the current analysis. When increasing the througput of this workflow however, retention time alignment protocols could be implemented to simplify data analysis.

The integrated OzID spectrum produced from the ions eluting at *ca.* 23.4 mins (Fig. 5C) contains two pairs of product ions at *m/z* 740 and 756 as well as *m/z* 700 and 716 that identify *n*-6 and *n*-9 double bonds on a common, polyunsaturated acyl chain. Based on information in both LC-OzID and LC-COzID experiments these ions can be attributed to PC 18:0/18:2(*n*-6, *n*-9), PC 18:2(*n*-6, *n*-9)/18:0 and PC 16:0/20:2(*n*-6, *n*-9). While the co-elution of these species means that the OzID spectrum shown in 5(C) represents a composite of the two acyl chain isomers (PC 18:0_18:2 and PC 16:0_20:2) the clear pattern of OzID product ions indicate that both species have identical unsaturation relative to the methyl termini of their respective acyl chains. The presence of both (*n*-6) species is consistent with elongation of diet derived 18:2(*n*-6) to form 20:2(*n*-6) in accordance with known metabolic pathways in humans. 39 Overall, the combination of LC-OzID and LC-COzID analysis identifies up to seven PC 36:2 isomers in RBC lipid extracts. The acquisition of the data in an LC-workflow dramatically reduced the spectral complexity (*cf.* direct infusion data in Fig. 1) and lessened the ambiguity in structural assignments.

3.3.3. Resolving lipid adduction isobars

Another advantage of introducing LC separation is reducing sample complexity by resolving adduct ion isobars. Analysis of LC-COzID data from red blood cell extracts obtained at *m/z* 808 and 810 revealed multiple features corresponding to isobars of different lipid composition. Representative data shown in Fig. 6 show the separate elution of different phosphatidylcholines that, when adducted with a proton or a sodium share a common precursor ion nominal mass. For example, [PC 38:5+H]$^+$ and [PC 36:2+Na]$^+$ at *m/z* 808.5 (Fig. 6A), and [PC 38:4+H]$^+$ and [PC 36:1+Na]$^+$ at *m/z* 810.5 (Fig. 6B) show clearly distinct retention time profiles. The XICs obtained from *m/z* 184 (produced by CID of protonated PC) and *m/z* 147 (produced by CID of sodiated PC) are shown in Fig. 6 and clearly demonstrate the separation of these lipids. The multiple features observed in the *m/z* 184 XICs are consistent with previous data identifying a range of isomers present for PC 38:5 and PC 38:4 [23,25,27,40].

3.3.4. Resolving lipid class isobars

Chromatographic separation of RBC lipid extracts also removed isobaric interference arising from different phospholipid classes, *e.g.*, [PC 38:3+Na]$^+$ and [PS 38:4+Na]$^+$ (*m/z* 834) as shown in Fig. 7(A). These data further serve to illustrate the ability of the COzID protocol to generate structural informative spectra from a complex lipid extract for PS lipids on a chromatographic time scale. The XIC of *m/z* 627 and 629 ions representing the loss of the sodiated headgroups from PS 38:4 and PC 38:3, respectively, were used to visualize the chromatographic features related to each lipid. Integration of the mass spectral data across both chromatographic features produced the COzID spectra shown in Fig. 7(B) and (C).

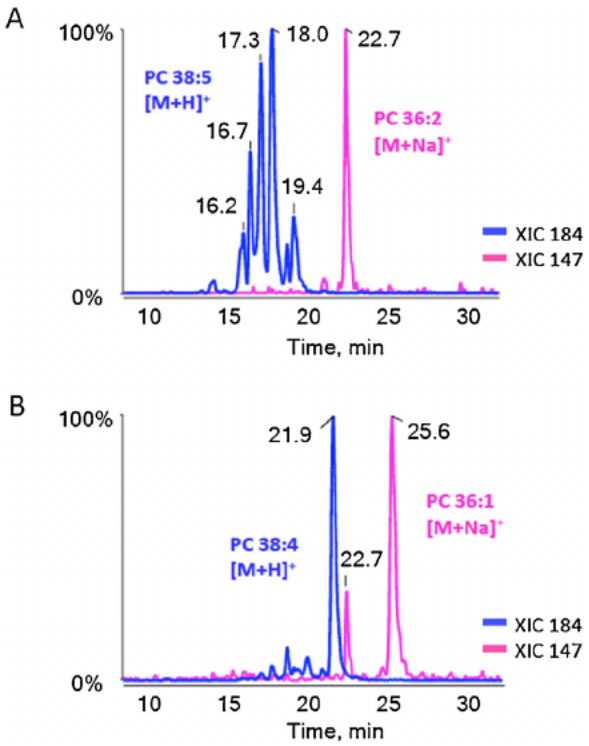

Fig. 6. UHPLC-COzID chromatograms for precursor ions of m/z 808 and 810 visualized using CID product ions m/z 184 and m/z 147 and show the resolution of isobaric overlap originating from different PC adduct ions. (A) $[PC38:5 + H]^+$ is separated from $[PC 36:2 + Na]^+$ and (B) $[PC 38:4 + H]^+$ is separated from $[PC 36:1 + Na]^+$ reducing interference seen in direct infusion analysis.

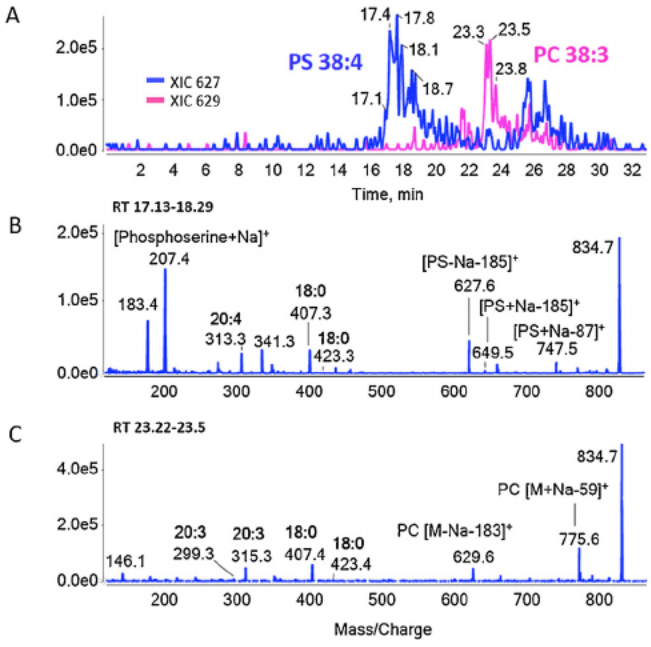

Fig. 7. (A) UHPLC-COzID chromatogram of a 5 μL injection of red blood cell extract trapping for m/z 834 ions. LC allowed separation of PS 38:4 from its isobaric PC 38:3 m/z 834 into different chromatographic features. XICs of CID product ions indicative of the loss of the sodiated phosphoserine headgroup m/z 627 (blue trace) vs m/z 627 (pink trace), which is diagnostic of the loss of the sodiated phosphocholine moiety. COzID mass spectra of the integrated chromatographic features between (B) 17.13-18.29 mins and (C) 23.22-23.5 mins are shown. (For interpretation of the references to colour in this figure legend, the reader is referred to the web version of this article.)

For the low mass ion in these spectra ($m/z < 250$), a slight mass shift is observed indicating poor mass calibration in this region. Nonetheless, ions m/z 146 and m/z 207 can be assigned as m/z 147 ($C_2H_5O_4NaP$) [35,36] and m/z 208 (sodiated phosphoserine moiety [Phosphoserine+Na]$^+$) [41], respectively and are indicative of the PS moiety. A loss of the serine moiety (–87 Da $C_3H_5NO_2$) [41] at m/z 747 is also observed, confirming the presence of a PS in this chromatographic feature. The COzID spectrum shown in Fig. 7(B) contains ions indicative of the presence of 18:0 at *sn*-1 (m/z 407 and 423) and 20:4 at *sn*-2 (m/z 297 and 313) that identify PS 18:0/20:4 the most abundant isomer eluting at *ca.* 17.8 min (see Supplementary Information, Table S4). In Fig. 7C, ions at m/z 775 and 629 represent neutral losses of 59 and 183 Da, respectively, that are indicative of a sodiated phosphatidylcholines [42] and confirm the presence of PC 38:3. COzID ions identify 18:0 at *sn*-1 (m/z 407 and 423) and 20:3 at *sn*-2 (m/z 299 and 315) further elucidating the identity of the lipid eluting at *ca.* 23.5 min as PC 18:0/20:3 (see Supporting Information, Tables S3 and S4). Notably, the signal-to-noise ratio is reduced for lower abundance lipid species (Fig. 7A) in contrast to high abundance lipids (Fig. 4A), however, the sensitivity of this workflow is demonstrated by its ability to generate COzID spectra capable of providing structural information for both PS and PC species (Fig. 7B and C). When combined with OzID analysis, the ion at m/z 834 can be identified as a cluster of isobars, *i.e.*, PC 38:3 and PS 38:4, and their respective double bond- and *sn*-positional isomers, specifically PC 18:0/20:3(*n*-6), PS 18:0/20:4(*n*-6) and PS 20:4(*n*-6)/18:0. This structural elucidation would have been difficult to ascertain for a complex lipid extract without LC separation.

4. Conclusions

The complexity of even ostensibly simple lipidomes, such as the human RBC analyzed here, results in the co-isolation of numerous lipids within the 1 Th isolation window afforded by modern mass spectrometers when utilising a shotgun approach. The resulting OzID spectra therefore contain fragment ions from each of the isolated lipids, complicating spectral interpretation. While combining CID and OzID is effective in obtaining near complete structural identification of phospholipids[14] it can further complicate spectra and impair the ability to identify low-abundance lipids. Here we present a new workflow utilising RP-UPLC to maximise isomer and isobar separation in combination with a 2-stage OzID and COzID protocol. This approach utilises serial LC runs with MS parameters optimized for either double bond ions (OzID) or *sn*-substitution ions (COzID) that are relatable, even with shifts in retention time. We were also able to reduce OzID reaction times allowing sufficient data within the LC timeframe. Additionally, a plug-in for Peakview™ software providing automated annotation of OzID spectra has been developed.

Application of this workflow to lipid extracts from human RBCs has provided new insight into the phospholipids present. For example, traditional CID of ions observed at m/z 834 in positive ion mode in a direct infusion experiment identifies the presence of both PC 38:3 and PS 38:4 as sodium adducts. The key diagnostic CID/OzID ions produced from these lipids are identical making it difficult to obtain a definitive structural characterization. The UPLC-OzID/COzID workflow allowed the unequivocal identification of PC 18:0/20:3(*n*-6), PS 18:0/20:4(*n*-6) and PS 20:4(*n*-6)/18:0, which was not possible using a direct injection approach. While the approach described here is not yet applicable to analysis of all lipids in a single high-throughput experiment it does allow detailed structure analysis of phospholipids, even at low concentration and can be applied across different lipid classes and tissues to provide the next step towards complete characterization of all phospholipids within complex lipidomes.

Acknowledgements:

This work was supported through funding from the *Australian Research Council* (ARC) Discovery Program (DP150101715). S.J.B. and T.W.M. are grateful for the support of SCIEX for this project through the ARC Linkage scheme (LP110200648).

Appendix A. Supplementary data

Supplementary data associated with this article can be found, in the online version, at https://doi.org/10.1016/j.ijms.2018.05.016.

References

[1] G. van Meer, D.R. Voelker, G.W. Feigenson, Membrane lipids: where they are and how they behave, Nat. Rev. Mol. Cell Biol. 9 (2) (2008) 112–124.
[2] M.R. Wenk, Lipidomics: new tools and applications, Cell 143 (6) (2010) 888–895.
[3] L. Yetukuri, K. Ekroos, A. Vidal-Puig, M. Oresic, Informatics and computational strategies for the study of lipids, Mol. Biosyst. 4 (2) (2008) 121–127.
[4] C. Bielow, G. Mastrobuoni, M. Orioli, S. Kempa, On mass ambiguities in high-Resolution shotgun lipidomics, Anal. Chem. 89 (5) (2017) 2986–2994.
[5] K. Ekroos, Lipidomics: Technologies and Applications, Wiley-VCH Verlag GmbH & Co., Germany, 2012.
[6] E. Ryan, G.E. Reid, Chemical derivatization and ultrahigh resolution and accurate mass spectrometry strategies for shotgun lipidome analysis, Accounts Chem. Res 49 (9) (2016) 1596–1604.
[7] S.E. Hancock, B.L. Poad, A. Batarseh, S.K. Abbott, T.W. Mitchell, Advances and unresolved challenges in the structural characterization of isomeric lipids, Anal. Biochem. 524 (2017) 45–55.
[8] S.H. Brown, T.W. Mitchell, S.J. Blanksby, Analysis of unsaturated lipids by ozone-induced dissociation, Biochim. Biophys. Acta. 1811 (11) (2011) 807–817.
[9] S.J. Blanksby, T.W. Mitchell, Advances in mass spectrometry for lipidomics, Ann. Rev. Anal. Chem. 3 (2010) 433–465.
[10] R. Almeida, J.K. Pauling, E. Sokol, H.K. Hannibal-Bach, C.S. Ejsing, Comprehensive lipidome analysis by shotgun lipidomics on a hybrid quadrupole-Orbitrap-Linear ion trap mass spectrometer, J. Am. Soc. Mass Spectrom. 26 (1) (2015) 133–148.
[11] D. Schwudke, K. Schuhmann, R. Herzog, S.R. Bornstein, A. Shevchenko, Shotgun lipidomics on high resolution mass spectrometers, Cold Spring Harb. Perspect. Biol 3 (9) (2011) a004614.
[12] B.L. Poad, H.T. Pham, M.C. Thomas, J.R. Nealon, J.L. Campbell, T.W. Mitchell, S.J. Blanksby, Ozone-induced dissociation on a modified tandem linear ion-trap: observations of different reactivity for isomeric lipids, Jornal of the American Society for Mass Spectrometry. 21 (12) (2010) 1989–1999.
[13] M.C. Thomas, T.W. Mitchell, D.G. Harman, J.M. Deeley, J.R. Nealon, S.J. Blanksby, Ozone-induced dissociation: elucidation of double bond position within mass-selected lipid ions, Anal. Chem. 80 (1) (2008) 303–311.
[14] H.T. Pham, A.T. Maccarone, M.C. Thomas, J.L. Campbell, T.W. Mitchell, S.J. Blanksby, Structural characterization of glycerophospholipids by combinations of ozone- and collision-induced dissociation mass spectrometry: the next step towards top-down lipidomics, Analyst 139 (1) (2014) 204–214.
[15] J.L. Campbell, T. Baba, Near-complete structural characterization of phosphatidylcholines using electron impact excitation of ions from organics, Anal. Chem. 87 (11) (2015) 5837–5845.
[16] X. Ma, L. Chong, R. Tian, R. Shi, T.Y. Hu, Z. Ouyang, Y. Xia, Identification and quantitation of lipid CC location isomers: a shotgun lipidomics approach enabled by photochemical reaction, Proc. Natl. Acad. Sci. U.S.A. 113 (10) (2016) 2573–2578.
[17] E. Ryan, C.Q.N. Nguyen, C. Shiea, G.E. Reid, Detailed structural characterization of sphingolipids via 193 nm ultraviolet photodissociation and ultra high resolution tandem mass spectrometry, J. Am. Soc. Mass Spectrom. 28 (7) (2017) 1406–1419.
[18] J.E. Kyle, X. Zhang, K.K. Weitz, M.E. Monroe, Y.M. Ibrahim, R.J. Moore, J. Cha, X. Sun, E.S. Lovelace, J. Wagoner, S.J. Polyak, T.O. Metz, S.K. Dey, R.D. Smith, K.E. Burnum-Johnson, E.S. Baker, Uncovering biologically significant lipid isomers with liquid chromatography, ion mobility spectrometry and mass spectrometry, Analyst 141 (5) (2016) 1649–1659.
[19] R.L. Kozlowski, J.L. Campbell, T.W. Mitchell, S.J. Blanksby, Combining liquid chromatography with ozone-induced dissociation for the separation and identification of phosphatidylcholine double bond isomers, Anal. Bioanal. Chem. 407 (17) (2015) 5053–5064.
[20] R.L. Kozlowski, T.W. Mitchell, S.J. Blanksby, Separation and identification of phosphatidylcholine regioisomers by combining liquid chromatography with a fusion of collision-and ozone-induced dissociation, Eur. J. Mass Spectrom. 21 (3) (2015) 191–200.
[21] B.L. Poad, M.R. Green, J.M. Kirk, N. Tomczyk, T.W. Mitchell, S.J. Blanksby, High-Pressure ozone-Induced dissociation for lipid structure elucidation on fast chromatographic timescales, Anal. Chem. 89 (7) (2017) 4223–4229.
[22] K. Ekroos, C.S. Ejsing, U. Bahr, M. Karas, K. Simons, A. Shevchenko, Charting molecular composition of phosphatidylcholines by fatty acid scanning and ion trap MS3 fragmentation, J. Lipid Res. 44 (11) (2003) 2181–2192.
[23] P. Koehrer, S. Saab, O. Berdeaux, R. Isaico, S. Gregoire, S. Cabaret, A.M. Bron, C.P. Creuzot-Garcher, L. Bretillon, N. Aca, Erythrocyte phospholipid and polyunsaturated fatty acid composition in diabetic retinopathy, PLoS One 9 (9) (2014) e106912.
[24] A. Sansone, E. Tolika, M. Louka, et al., Hexadecenoic fatty acid isomers in human blood lipids and their relevance for the interpretation of lipidomic profiles, PLoS One 11 (4) (2016) e0152378.
[25] O. Uhl, H. Demmelmair, M. Klingler, B. Koletzko, Changes of molecular glycerophospholipid species in plasma and red blood cells during docosahexaenoic acid supplementation, Lipids 48 (11) (2013) 1103–1113.
[26] G.P. Amminger, M.R. Schafer, K. Papageorgiou, et al., Long-chain omega-3 fatty acids for indicated prevention of psychotic disorders: a randomized, placebo-controlled trial, Arch. Gen. Psychiatry 67 (2) (2010) 146–154.
[27] W.E. Connor, D.S. Lin, G. Thomas, F. Ey, T. DeLoughery, N. Zhu, Abnormal phospholipid molecular species of erythrocytes in sickle cell anemia, J. Lipid Res. 38 (12) (1997) 2516–2528.
[28] C. von Schacky, Use of red blood cell fatty-acid profiles as biomarkers in cardiac disease, Biomark. Med. 3 (1) (2009) 25–32.
[29] V. Matyash, G. Liebisch, T.V. Kurzchalia, A. Shevchenko, D. Schwudke, Lipid extraction by methyl-tert-butyl ether for high-throughput lipidomics, J. Lipid Res. 49 (5) (2008) 1137–1146.
[30] A. Alqarni, S.H. Brown, B.J. Meyer, T.W. Mitchell. A validated high throughput method for the analysis of erythrocyte fatty acids and the omega-3 index 2018-Submitted.
[31] A.T. Maccarone, J. Duldig, T.W. Mitchell, S.J. Blanksby, E. Duchoslav, J.L. Campbell, Characterization of acyl chain position in unsaturated phosphatidylcholines using differential mobility-mass spectrometry, J. Lipid Res. 55 (8) (2014) 1668–1677.
[32] E. Fahy, S. Subramaniam, R.C. Murphy, et al., Update of the LIPID MAPS comprehensive classification system for lipids, J. Lipid Res 50 (Suppl) (2009) S9–14.
[33] G. Liebisch, J.A. Vizcaino, H. Kofeler, et al., Shorthand notation for lipid structures derived from mass spectrometry, J. Lipid Res. 54 (6) (2013) 1523–1530.
[34] The nomenclature of lipids (Recommendations 1976) IUPAC-IUB commission on biochemical nomenclature, Biochem. J. 171 (1) (1978) 21–35.
[35] K.A. Al-Saad, W.F. Siems, H.H. Hill, V. Zabrouskov, N.R. Knowles, Structural analysis of phosphatidylcholines by post-source decay matrix-assisted laser desorption/ionization time-of-flight mass spectrometry, J. Am. Soc. Mass Spectrom. 14 (4) (2003) 373–382.
[36] X. Han, R.W. Gross, Structural determination of lysophospholipid regioisomers by electrospray ionization tandem mass spectrometry, J. Am. Chem. Soc. 118 (1996) 451–457.
[37] R.C. Murphy, Tandem Mass Spectrometry of Lipids: Molecular Analysis of Complex Lipids, Royal Society of Chemistry, Cambridge, U.K, 2014.
[38] M.C. Thomas, T.W. Mitchell, S.J. Blanksby, OnLine ozonolysis methods for the determination of double bond position in unsaturated lipids, Methods Mol. Biol. 579 (2009) 413–441.
[39] H. Guillou, D. Zadravec, P.G.P. Martin, A. Jacobsson, The key roles of elongases and desaturases in mammalian fatty acid metabolism: insights from transgenic mice, Prog. lipid Res. 49 (2) (2010) 186–199.
[40] D. Pacetti, R. Gagliardi, M. Balzano, N.G. Frega, M.L. Ojeda, M. Borrero, A. Ruiz, P. Lucci, Changes in the fatty acid profile and phospholipid molecular species composition of human erythrocyte membranes after hybrid palm and extra virgin olive oil supplementation, J. Agric. Food Chem. 64 (27) (2016) 5499–5507.
[41] F.F. Hsu, J. Turk, Studies on phosphatidylserine by tandem quadrupole and multiple stage quadrupole ion-trap mass spectrometry with electrospray ionization: structural characterization and the fragmentation processes, J. Am. Soc. Mass Spectrom. 16 (9) (2005) 1510–1522.
[42] F.F. Hsu, J. Turk, Electrospray ionization/tandem quadrupole mass spectrometric studies on phosphatidylcholines: the fragmentation processes, J. Am. Soc. Mass Spectrom. 14 (4) (2003) 352–363.